Role of Extracellular Polymeric Substances (EPS) in Biofouling of Reverse Osmosis Membranes

ARTICLE *in* ENVIRONMENTAL SCIENCE AND TECHNOLOGY · JULY 2009

Impact Factor: 5.33 · DOI: 10.1021/es900087j · Source: PubMed

3 AUTHORS:

Moshe Herzberg
Ben-Gurion University of the Negev
54 PUBLICATIONS **1,677** CITATIONS
SEE PROFILE

Seoktae Kang
Kyung Hee University
53 PUBLICATIONS **2,870** CITATIONS
SEE PROFILE

Menachem Elimelech
Yale University
395 PUBLICATIONS **32,645** CITATIONS
SEE PROFILE

Role of Extracellular Polymeric Substances (EPS) in Biofouling of Reverse Osmosis Membranes

MOSHE HERZBERG,*,† SEOKTAE KANG,‡ AND MENACHEM ELIMELECH‡

Department of Desalination and Water Treatment, Zuckerberg Institute for Water Research, Ben-Gurion University of the Negev, Sede Boqer Campus 84990, Israel, and Department of Chemical Engineering, Environmental Engineering Program, Yale University, New Haven, Connecticut 06520-8286

Received January 11, 2009. Revised manuscript received April 16, 2009. Accepted April 17, 2009.

This study elucidates the mechanisms by which extracellular polymeric substances (EPS) impact permeate water flux and salt rejection during biofouling of reverse osmosis (RO) membranes. RO fouling experiments were conducted with *Pseudomonas aeruginosa* PAO1, EPS extracted from PAO1 biofilms, and dead PAO1 cells fixed in formaldehyde. While a biofouling layer of dead bacterial cells decreases salt rejection and permeate flux by a biofilm-enhanced osmotic pressure mechanism, the EPS biofouling layer adversely impacts permeate flux by increasing the hydraulic resistance to permeate flow. During controlled fouling experiments with extracted EPS in a simulated wastewater solution, polysaccharides adsorbed on the RO membranes much more effectively than proteins (adsorption efficiencies of 61.2−88.7% and 11.6−12.4% for polysaccharides and proteins, respectively). Controlled fouling experiments with EPS in sodium chloride solutions supplemented with 0.5 mM calcium ions (total ionic strength of 15 mM) indicate that calcium increases the adsorption efficiency of polysaccharides and DNA by 2- and 3-fold, respectively. The increased adsorption of EPS onto the membrane resulted in a significant decrease in permeate water flux. Corroborating with these calcium effects, atomic force microscopy (AFM) measurements demonstrated that addition of calcium ions to the feed solution results in a marked increase in the adhesion forces between a carboxylated particle probe and the EPS layer. The increase in the interfacial adhesion forces is attributed to specific EPS-calcium interactions that play a major role in biofouling of RO membranes.

Introduction

The impairment of reverse osmosis (RO) membrane performance due to fouling represents a formidable challenge in advanced reclamation of wastewater effluents and in seawater desalination (*1*−*4*). The most common adverse effects of biofouling include a decline in RO permeate flux and a decrease in salt rejection (*5, 6*). Furthermore, frequent chemical cleaning for fouling control shortens membrane life and produces waste streams that need to be disposed of. Foulants of RO membranes typically comprise sparingly soluble inorganic salts, as well as organic, colloidal, and microbiological matter. While organic foulants and scaling on the membrane surface increase the hydraulic resistance to permeate flux, colloidal fouling and bacterial cells reduce permeate flux via a cake- and biofilm-enhanced osmotic pressure (CEOP and BEOP) mechanism that leads to increased transmembrane osmotic pressure (*7*−*11*).

Organic fouling of salt rejecting membranes (i.e., reverse osmosis and nanofiltration) has been studied extensively over the past decade. Among the factors that govern the fouling of such membranes are (i) membrane surface properties, including hydrophobicity, charge, and surface roughness (*12*−*14*); (ii) foulant properties, such as molecular weight and polarity (*15, 16*); (iii) source water chemistry (pH, divalent cations, and salinity) (*17*−*21*); and (iv) operating conditions (permeate flux, applied pressure, and crossflow hydrodynamics) (*21, 22*). In general, surfaces that are most likely to resist organic fouling are characterized as being hydrophilic, H-bond acceptors, non-H-bond donors, and neutrally charged surfaces (*3, 23, 24*). Rougher and more hydrophobic membranes have a higher tendency for fouling by natural organic matter (NOM) and soluble microbial products (SMP) (*25*). In most cases, enhanced NOM fouling is observed in the presence of divalent cations, high ionic strength, and low pH (*26*). In addition, NOM and SMP components are differentially adsorbed to membranes during fouling. In experiments with both NOM and SMP as foulants, polysaccharides were reported to preferentially adsorb to nanofiltration (NF) membranes (*27*).

As the adhesive and cohesive matrix of biofilms, extracellular polymeric substances (EPS) play an important role in controlling the permeate water flux decline in membrane processes. For example, Fonseca et al. (*27*) showed that NF permeate flux decline during biofouling correlated to the membrane-associated EPS content. For RO membranes, it was proposed that EPS reduce turbulent flow in close proximity to the membrane surface, leading to elevated concentration polarization and subsequent permeate flux decline (*28*). A recent study modeling mass transfer in RO biofilms suggested that both the void fraction in the biofilm and the partitioning of solutes at the EPS-voids interface could hinder the back-diffusion of solutes and eventually increase the transmembrane osmotic pressure (*29*).

In experiments examining fouling of RO membranes with alginate as a surrogate for EPS, calcium was found to severely decrease permeate flux by the formation of a compact impermeable fouling layer (*19*). Fouling of RO and NF membranes with bovine serum albumin (BSA) and alginate, as model protein and polysaccharide, respectively, was recently reported to be affected by membrane surface roughness, with a synergistic fouling effect for a mixture of the two model compounds (*17, 30*). Alginate was found to foul the RO membrane more severely than BSA, exhibiting a much more pronounced effect in the presence of calcium. However, these studies with model biomacromolecules representing major EPS components cannot adequately simulate the complex nature of bacterial EPS and the overall process of biofouling of RO membranes.

The mechanisms of biofouling and the specific contributions of the various biofilm components, especially EPS, to the deterioration of RO membrane performance are not well understood. In our previous study on RO biofouling, bacterial cells were found to enhance concentration polarization, thereby suggesting that EPS contribute mainly to increased hydraulic resistance (*9*). In this paper, we systematically investigate the contribution of EPS to the biofouling of RO

* Corresponding author phone: +972-8-6563520; e-mail: herzberg@bgu.ac.il.
† Ben-Gurion University of the Negev.
‡ Yale University.

10.1021/es900087j CCC: $40.75
Published on Web 05/07/2009

membranes and relate the fouling mechanisms to the major EPS components. Physicochemical interactions and fouling mechanisms of EPS are characterized by analyzing the major EPS components retained on the membrane surface, monitoring the decline in permeate flux and salt rejection behavior, and measuring the interfacial adhesion forces among EPS.

Materials and Methods

Model Bacterial Strain and Media. *Pseudomonas aeruginosa* PAO1 was used as the model bacterium for the enhanced biofouling experiments. A fresh single colony of *P. aeruginosa* PAO1 was grown in LB medium and harvested at exponential growth phase to serve as the inoculum for the biofouling experiments. An enriched synthetic wastewater solution was used as the bacterial growth medium to accelerate the biofilm growth on the RO membranes. The synthetic wastewater medium was supplemented with a relatively high concentration of carbon (as citrate) and with a small amount of LB broth (1:1000 dilution). The chemical composition of the synthetic wastewater was based on secondary effluent quality from selected wastewater treatment plants in California as described in our recent publication (*9*). The final pH of the synthetic wastewater was 7.4 and the calculated ionic strength was 14.6 mM.

EPS Extraction and Preparation. EPS were extracted from a biofilm culture of *P. aeruginosa* PAO1 cultivated with 20 g of untreated glass wool fibers (Corning Glass Works, Corning, NY) in 500 mL of LB using a modified version of the Liu and Fang method (*31*). After the extraction, the EPS solution was filtered through a 0.2-μm hydrophilic nylon filter (Millipore) and dialyzed through a membrane with a molecular weight cutoff of 3500 Da (Spectra/Por). Finally, a 50-mL sample of resuspended EPS solution was lyophilized at -50 °C under vacuum (0.01 mbar) to facilitate determination of dry weight concentration. Two batches of EPS were produced and used for the fouling experiments. EPS that accumulated on the RO membrane during fouling runs were obtained by scraping the layer with a spatula and vortexing the RO membrane coupon for 10 min in DI water.

RO Membrane and Crossflow Test Unit. The model membrane for the fouling experiments was a commercial thin-film composite RO membrane, LFC-1 (Hydranautics, Oceanside, CA). The hydraulic resistance of the membrane was $1.06 \pm 0.02 \times 10^{14}$ m^{-1} at 25 °C and the observed salt rejection was 97.89 ± 0.44%, determined using the synthetic wastewater solution at an applied pressure of 180 psi (12.4 bar) and a crossflow velocity of 8.5 cm/s. The physical and chemical properties of the LFC-1 membrane and detailed description of the RO test unit are described in our previous publications (*9, 32*).

Biofouling Protocols. The RO unit was disinfected and cleaned prior to the fouling experiments with live biofilm, EPS, or fixed dead cells as described by Herzberg et al. (*9*). Biofilm growth on the RO membrane was initiated according to our previously published biofouling protocol (*9, 33*). The protocol for fouling the RO membrane with EPS was similar, with the exception that EPS stock solution was added to the RO unit after 5 h of equilibration, with the salts and organics comprising the synthetic wastewater medium. The EPS stock solution was supplemented with the same background salt solution as that used during the enhanced biofouling experiments (i.e., synthetic wastewater solution). Final EPS feed concentration in the RO fouling tests was set to 8 mg/L as dissolved organic carbon (DOC). For analyzing the influence of calcium on fouling with EPS, fouling experiments were conducted in NaCl solutions with and without the addition of 0.5 mM $CaCl_2$. The total ionic strength was fixed at 15 mM and the ambient pH was 6.1. Fouling of the RO membrane with dead cells was performed after fixation of the cells with a 4% buffered formaldehyde solution at pH 6.6 and washing the cells according to the protocol described in our previous study (*9*).

EPS Component Analysis. Polysaccharide content in the EPS was analyzed colorimetrically according to Dubois et al. (*34*) with sodium alginate as the standard (10−100 mg/L) Total protein content in the EPS was analyzed by using a modified Lowry protein assay kit (Pierce, Rockford, IL) according to Frolund et al. (*35*). DNA was analyzed by hybridization of 4′,6-diamidino-2-phenylindole (DAPI) to the nucleic acids in the EPS. Salmon sperm DNA (Invitrogen) was used as the standard (0−168 ng/mL).

Adhesion Force Measurements. A Nanoscope III Multimode AFM (Digital Instruments, Santa Barbara, CA) was used to quantify the adhesion forces between a carboxylate-modified latex (CML) particle (Interfacial Dynamics Corp., Portland, OR) and membranes fouled with EPS, taken at the end of the fouling experiment. The CML particle, 3 μm in diameter, was glued to the end of a commercial 0.06 N/m SiN tipless cantilever (Veeco Metrology Group, Santa Barbara, CA) and was used as a surrogate for EPS because it carries predominantly carboxylic functional groups. The AFM was operated in a force mode, with an approach/retraction speed of 1 μm/s and 1 μm of piezo movement. The experiments were performed in a liquid cell, allowing the system to equilibrate for 60 min for each experimental condition. Raw data were converted from cantilever deflection and z-piezo position into force—distance curves. The force was then normalized by the radius of the CML particle, R. For a given system, F/R serves as an indicator for the membrane fouling potential (*19, 20*). Detailed experimental procedures for using the AFM colloid-probe technique to quantify interaction forces relevant to organic fouling are given in our previous publications (*19, 20, 23*). Force measurements were performed at four different locations on the membrane surface, with 15 measurements at each location to minimize inherent variability in the force data. The chemical compositions of the test solutions in the liquid cell were the same as those used in the fouling experiments.

Results and Discussion

Biofouling Adversely Impacts Membrane Permeate Flux and Salt Rejection. Formation of a *P. aeruginosa* PAO1 biofilm on the RO membrane resulted in a decrease of both the RO permeate water flux and salt rejection (Supporting Information (SI), Figure S1), as observed in our previous study (*9*). The mechanisms responsible for the decline in permeate flux include an increase in the hydraulic resistance of the fouled membrane and a simultaneous increase in the transmembrane osmotic pressure due to hindered back-diffusion of salt in the biofilm. This biofilm-enhanced osmotic pressure (BEOP) mechanism originates from the bacterial cell component of the biofilm (*9*) and is the main cause of the decrease in salt rejection from 98.2 to 93.6% (SI Figure S1). Similar observations of enhanced osmotic pressure were demonstrated when colloidal cake layers formed on RO membranes (*7, 8*).

Relative Roles of Hydraulic Resistance and Transmembrane Osmotic Pressure. Figure 1 presents fouling experiments with fixed dead *P. aeruginosa* PAO1 cells and their isolated EPS under similar conditions. In order to analyze the hydraulic resistance of the EPS and fixed dead cell layers, and to eliminate concentration polarization effects, fouling experiments were conducted using a background solution of DI water with a minor concentration (0.01 mM) of lanthanum chloride ($LaCl_3$). A minimal dose of $LaCl_3$ is required to enhance the adsorption/accumulation of negatively charged macromolecules and particles onto the RO membrane to overcome repulsive forces that otherwise would be substantial with DI water alone (*7*). This very low concentration of $LaCl_3$ does not produce measurable osmotic

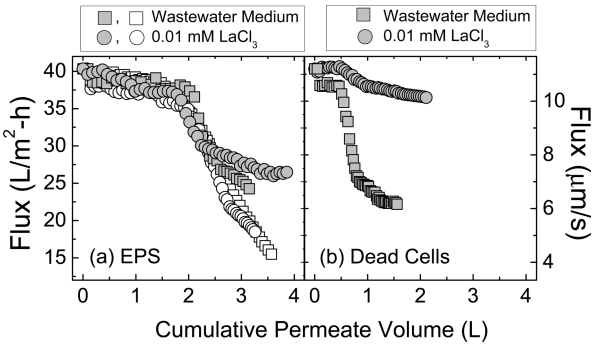

FIGURE 1. RO permeate flux behavior as a function of cumulative permeate volume for fouling runs with (a) two batches of EPS (extracted from a biofilm of *P. aeruginosa* PAO1) and (b) formaldehyde-fixed dead *P. aeruginosa* PAO1 cells (initial concentration of 10^9 cells per mL). Fouling experiments were conducted with a synthetic wastewater medium (ionic strength of 14.6 mM and pH 7.4) or with deionized water supplemented with 0.01 mM $LaCl_3$ (pH 5.8) as indicated. Initial EPS concentration was 8 mg/L as DOC, crossflow velocity was 8.5 cm/s, and the temperature was fixed at 25 °C. At the end of the EPS fouling runs, the cumulative volume range of 3.2−3.9 L corresponds to 46.8−59.9 h of filtration. At the end of the fouling runs with dead cells, the cumulative volumes of 1.6 and 2.1 L correspond to 27.8 and 27.4 h of filtration, respectively. Note that the membrane surface area is 2.00 × 10^{-3} m^2.

pressure at the membrane surface, thereby enabling the determination of the hydraulic resistance of the cake layer formed by dead cells or EPS.

The fouling experiments with DI water supplemented with 0.01 mM $LaCl_3$ (pH 5.8) were compared to similar experiments with wastewater media (ionic strength of 14.6 mM and pH 7.4). When the membrane was fouled with the fixed dead cells, only a minor decrease in permeate flux was observed when the solution contained 0.01 mM $LaCl_3$ (Figure 1b), thereby indicating a minimal hydraulic resistance of the fouling layer comprising the bacteria. However, in the presence of salts in the wastewater medium, a drastic decline in permeate flux was observed due to the increase in the transmembrane osmotic pressure. In contrast to the case of fouling the RO membrane with a cake layer of dead cells, when EPS were used as the fouling agent, the decrease in permeate flux in the synthetic wastewater experiment was similar to that observed in the 0.01 mM $LaCl_3$ solution experiment. This observation indicates that induced hydraulic resistance, rather than enhanced concentration polarization, was responsible for the permeate flux decline with EPS (Figure 1a).

Salt rejection of clean membranes at the beginning of the EPS fouling experiments varied between 98.2 and 99.0%, while at the end of these experiments, salt rejection decreased to 97.1 and 96.6% in batches 1 and 2 of EPS, respectively. This decrease in salt rejection is attributed to a "concentration effect" of the salts in the permeate due to reduced permeate flux, as verified in a series of experiments with a clean membrane over a range of applied pressures and associated water fluxes (Figure 2). The observed salt rejection at low water fluxes, comparable to those at the end of the EPS fouling runs, was only slightly higher than the salt rejection observed at the end of the fouling experiments with EPS. In contrast, the much greater decrease in salt rejection for fouling by a cake layer of dead cells cannot be explained by a permeate flux decline or concentration effect. This decrease in salt rejection is attributed mainly to a hindered back-diffusion of salts in the thick layer of dead cells, thereby increasing the salt concentration at the membrane surface.

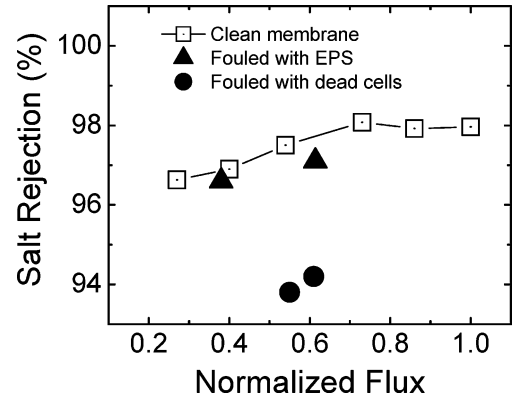

FIGURE 2. Dependence of salt rejection on permeate flux to examine the "concentration effect" of salts in the product water upon reduction in permeate flux. The permeate flux was changed from its initial value by subsequent reductions in the applied hydraulic pressure. A clean RO membrane was used with a synthetic wastewater medium (ionic strength of 14.6 and pH 7.4). Permeate flux was changed every 4 h. The initial permeate flux was 1.17 (±0.06) × 10^{-5} m/s (42.1 L/m^2-h or 24.8 gal/ft^2-day), crossflow velocity was 8.5 cm/s, and temperature was fixed at 25 °C.

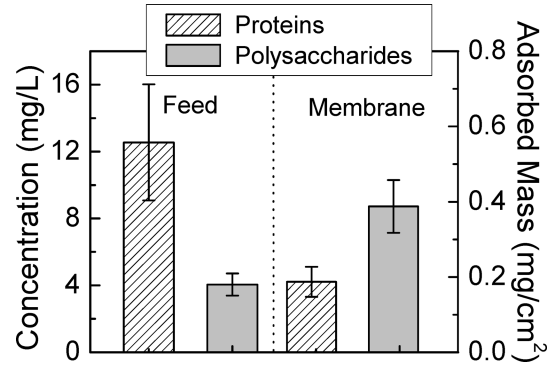

FIGURE 3. Concentrations of proteins and polysaccharides in the feed solution (mg/L) and on the fouled RO membrane (mg/cm^2). The results represent the average of the experiments with the two batches of EPS for the fouling runs depicted in Figure 1. Initial EPS concentration was 8 mg/L as DOC (in synthetic wastewater medium), crossflow velocity was 8.5 cm/s, and the temperature was fixed at 25 °C.

Adsorption of EPS Main Components. To obtain further insight into EPS adsorption and fouling mechanisms, EPS composition was analyzed both in the bulk (feed) solution and for the RO membrane fouling layer. EPS comprise a variety of biomacromolecules, primarily proteins and polysaccharides, as well as other components, such as lipids and DNA, that may have a significant influence on the physicochemical properties of the biofouling layer (*28, 35*). EPS composition in the bulk solution of the RO unit does not necessarily reflect the EPS composition on the RO membrane due to different adsorption rates of the EPS components onto the membrane. Our findings demonstrated the preferential adsorption/accumulation of polysaccharides on the EPS fouling layer. While protein concentration in the EPS feed solution was 3-fold higher than that of the polysaccharides, the trend was reversed in the EPS fouling layer (Figure 3). Furthermore, DNA concentrations in the EPS feed solution were 0.036 ± 0.006 and 0.033 ± 0.008 mg/L for batches 1 and 2, respectively, whereas after fouling the corresponding amounts in the fouling layers were 2.6 ± 0.055 and 1.7 ± 0.061 $\mu g/cm^2$, respectively.

Quantitative analysis of EPS components in solution and on the membrane surface underscores the preferential

TABLE 1. Amounts of EPS Components in the Bulk (Feed) Solution and Adsorbed Fouling Layer

	wastewater medium, batch 1	wastewater medium, batch 2	NaCl, IS = 15 mM	NaCl + 0.5 mM Ca^{2+}, IS = 15 mM
EPS				
initial dissolved EPS (mg/L) (8 mg/L as TOC)	20 ± 4.8	24 ± 5.5	22 ± 6.9	22 ± 6.9
adsorbed EPS (mg/cm^2)	0.65 ± 0.20	0.89 ± 0.29	0.36 ± 0.14	0.55 ± 0.17
calculated max. adsorbed EPS (mg/cm^2)	2.65	2.86	3.41	3.50
adsorption efficiency (%)	24.5 ± 7.5	31.1 ± 10.1	10.6 ± 4.1	15.7 ± 4.9
Proteins				
initial dissolved proteins (mg/L)	10.1 ± 2.2	15.0 ± 0.92	12.55 ± 2.83	12.55 ± 2.83
adsorbed proteins (mg/cm^2)	0.15 ± 0.029	0.22 ± 0.064	0.10 ± 0.021	0.12 ± 0.026
calculated max. adsorbed proteins (mg/cm^2)	1.29	1.77	1.95	1.99
adsorption efficiency (%)	11.6 ± 2.2	12.4 ± 3.6	5.1 ± 1.1	5.0 ± 1.1
Polysaccharides				
initial dissolved polysaccharides (mg/L)	3.6 ± 0.3	4.51 ± 0.4	4.05 ± 0.49	4.05 ± 0.49
adsorbed polysaccharides (mg/cm^2)	0.30 ± 0.056	0.47 ± 0.096	0.14 ± 0.005	0.27 ± 0.015
calculated max. adsorbed polysaccharides (mg/cm^2)	0.49	0.53	0.63	0.64
adsorption efficiency (%)	61.2 ± 11.4	88.3 ± 18.1	22.2 ± 0.8	42.2 ± 2.3
DNA				
initial dissolved DNA (mg/L)	0.0359 ± 0.0059	0.033 ± 0.008	0.034 ± 0.01	0.034 ± 0.01
adsorbed DNA (μg/cm^2)	2.6 ± 0.055	1.7 ± 0.061	0.11 ± 0.06	0.36 ± 0.05
calculated max. adsorbed DNA (μg/cm^2)	4.6	3.9	0.54	0.55
adsorption efficiency (%)	56.5 ± 1.2	43.6 ± 1.6	20.4 ± 11.1	65.4 ± 9.02

adsorption/accumulation of polysaccharides in the fouling layer. The maximum theoretical mass for EPS adsorption, $M(t)$, during the fouling experiment can be calculated assuming that each EPS component is transported to the membrane by the convective permeate flow and completely adsorbs to the fouling layer. $M(t)$ and the bulk foulant concentration, $C_{foulant}(t)$, were calculated at each time corresponding to the permeate flux, $J(t)$, from

$$M(t) = \int_0^t C_{foulant}(t)J(t)A\mathrm{d}t \quad (1)$$

$$C_{foulant}(t) = C_{foulant}(t=0) - \mathrm{M}(t)/V \quad (2)$$

Here, A is the membrane surface area, t is the time, and V is the bulk solution volume of the RO unit. The maximum adsorbed mass at the end of the fouling run is calculated by integration of eq 1 for the entire fouling run. The actual (measured) mass adsorbed on the RO membranes, the maximum theoretical adsorbed mass, and the adsorption efficiency (the actual adsorbed mass divided by maximum theoretical mass) for each EPS component, as well as the initial dissolved concentration of the EPS and its components, for the fouling experiments, are summarized in Table 1. As seen, adsorption efficiency for polysaccharides (61.2 ± 11.4% and 88.7 ± 18.1%) was much higher than that of proteins (11.6 ± 2.2% and 12.4 ± 3.6%) in the synthetic wastewater medium. DNA adsorption efficiency was relatively high and reached values between 43.6 ± 1.6% and 56.5 ± 1.2%. Discussion on the preferential adsorption of polysaccharides onto the RO membrane is given in the following subsections.

Influence of Calcium on EPS Fouling. Polysaccharide-calcium specific interactions have a major effect on the mechanical stability of biofilms (*36*) and on organic fouling of RO membranes (*19, 37*). EPS fouling experiments were conducted in the presence and absence of calcium ions (0.5 mM) in NaCl solutions adjusted to an ionic strength of 15 mM. A greater permeate flux decline was observed with the EPS solution supplemented with calcium (Figure 4a). The normalized permeate flux at the end of the fouling run was 0.67 in the presence of calcium ions, while that in the absence of calcium ions was 0.78. A minor decrease in salt rejection was observed at the end of the fouling experiments, from 98.5% and 98.3% to 97.1% and 97.6% with and without calcium, respectively. This decrease in salt rejection is likely attributed to the decrease in permeate flux and to the associated concentration effect, as observed in the previous EPS fouling experiments and verified with experiments using a clean membrane (Figure 2).

Calcium ions also resulted in preferential adsorption of polysaccharides (Figure 4b) and DNA (Table 1) onto the RO

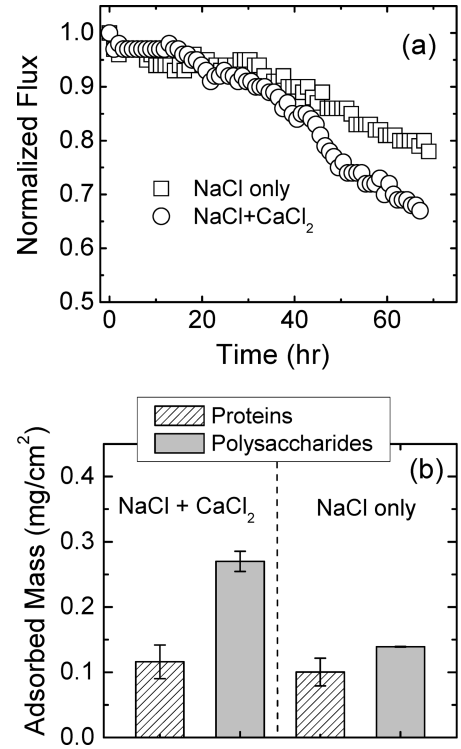

FIGURE 4. Effect of calcium ions on EPS fouling propensity and adsorption/accumulation on the RO membrane fouling layer: (a) normalized permeate flux decline during the filtration of EPS solution (8 mg/L as DOC) and (b) protein and polysaccharide concentrations on the membrane fouling layers. Fouling experiments were conducted with NaCl solutions with and without 0.5 mM $CaCl_2$. The total ionic strength was adjusted to 15 mM at an ambient pH of 6.1. The initial permeate flux was 1.19 (±0.06) × 10^{-5} m/s (42.8 L/m^2-h or 25.2 gal/ft^2-day), crossflow velocity was 8.5 cm/s, and temperature was fixed at 25 °C.

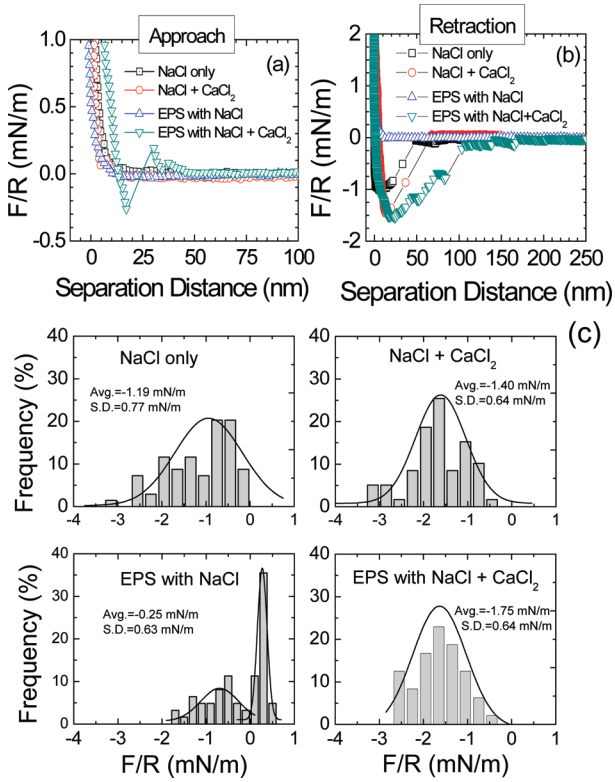

FIGURE 5. The effect of calcium ions on the interaction forces between the CML particle probe and EPS-fouled RO membrane surface. (a) Representative interaction forces (approach curves), (b) representative adhesion (retraction) force curves, and (c) distribution of the maximum adhesion forces between the CML particle and the membrane with NaCl solutions with and without 0.5 mM $CaCl_2$ (total ionic strength adjusted to 15 mM at ambient pH of 6.2). EPS concentration used was 8 mg/L as DOC and the temperature was fixed at 25 °C.

membrane. The presence of calcium increased the total mass of EPS adsorbed on the RO membrane surface (Table 1) as well as the adsorption of each of the EPS components (Table 1 and Figure 4b). The increase in total mass of adsorbed EPS is mainly due to the higher adsorption efficiency of polysaccharides in the presence of calcium. As shown in Figure 4b, the amount of polysaccharides adsorbed on the RO membrane was doubled in the presence of calcium ions, while that of proteins was not changed. Thus, the permeate flux decline in the presence of calcium ions was mainly due to the increase in the adsorption of polysaccharides.

A number of studies have shown calcium to be a major cause of enhanced fouling with NOM or model polysaccharides such as alginate and dextran (*19, 20, 26, 38*). Similarly, other studies have shown enhancement in membrane fouling with BSA in the presence of calcium, though less significantly than membrane fouling with alginate (*17, 19*). In the current study, calcium "finger printing" was also reflected in the increased adsorption efficiency of extracellular DNA. Adsorption efficiencies of the extracellular DNA increased from 20.4 ± 11.1% with no calcium to 65.4 ± 9.02% with calcium (Table 1). The higher adsorption efficiency of DNA in the presence of calcium can be explained by either cationic bridging or by calcium adsorption to the negatively charged phosphate backbone of the DNA molecules and subsequent charge neutralization (*39*).

Interfacial Adhesion Forces. Our previous studies demonstrated that atomic force microscopy allows both quantitative measurement of adhesion forces and qualitative understanding of foulant−membrane and foulant−foulant interactions during membrane fouling (*19, 23, 37*). We have also shown that the normalized adhesion force, F/R, serves as an indicator for the fouling propensity of polymeric membranes (*19, 20*).

Normalized interaction force curves during the approach of a CML particle probe to the membrane surface, with an EPS-free solution, showed purely repulsive forces in the presence and absence of calcium ions due to significant electrostatic double layer repulsion at 15 mM ionic strength (Figure 5a). However, in the presence of EPS in solution, attractive "jump-in" forces were frequently observed during the approach events when calcium ions were added (Figure 5a). These jump-in events indicate bridging between the EPS and the CML probe due to the complexation or binding of calcium ions to carboxylic groups. Similar attractive events due to calcium bridging were reported for a CML particle probe interacting with an NF membrane in the presence of humic acid (*20*).

Retraction force curves, presented as F/R versus separation distance from the fouled membrane (Figure 5b) or distribution of maximum adhesion forces (Figure 5c), reflect more dramatically the important effect of calcium ions on EPS fouling. When the solution was supplemented with calcium ions, a marked increase in the adhesion force was observed upon retraction of the CML probe from the EPS fouled membrane. The AFM force measurements clearly showed that the force profiles during the retraction of the CML probe were more attractive when calcium ions were present in the solution, with and without EPS. The increase in the adhesion forces is attributed to specific interactions of calcium ions with EPS carboxylic groups. The majority of the carboxylic groups are likely those of polysaccharides that become the more dominant fraction in the fouling layer in the presence of calcium ions (Figure 4b). Notably, very weak adhesion forces as well as no adhesion (indicated by F/R equal or greater than zero) were observed upon retraction of the CML probe in the absence of calcium (Figure 5c). These results are attributable to a combination of the negative charge of both the CML particle probe and the EPS fouling layer and the relatively high hydrophilicity of the EPS fouling layer.

Acknowledgments

This research was made possible by the WaterCAMPWS, a Science and Technology Center of Advanced Materials for the Purification of Water with Systems under the National Science Foundation agreement number CTS-0120978, and by a postdoctoral fellowship supplied by the United States-Israel Binational Agricultural Research and Development (BARD) fund.

Supporting Information Available

Permeate flux and salt rejection upon growth of a *P. aeruginosa* PAO1 biofilm on an RO membrane (Figure S1). This material is available free of charge via the Internet at http://pubs.acs.org.

Literature Cited

(1) Chen, K. L.; Song, L.; Ong, S. L.; Ng, W. J. The development of membrane fouling in full-scale RO processes. *J. Membr. Sci.* **2004**, *232*, 63–72.
(2) Jarusutthirak, C.; Amy, G. Role of soluble microbial products (SMP) in membrane fouling and flux decline. *Environ. Sci. Technol.* **2006**, *40*, 969–974.
(3) Shannon, M. A.; Bohn, P. W.; Elimelech, M.; Georgiadis, J. G.; Marinas, B. J.; Mayes, A. M. Science and technology for water purification in the coming decades. *Nature* **2008**, *452*, 301–310.
(4) Xu, P.; Drewes, J. E.; Kim, T.-U.; Bellona, C.; Amy, G. Effect of membrane fouling on transport of organic contaminants in NF/RO membrane applications. *J. Membr. Sci.* **2006**, *279*, 165–175.

(5) Flemming, H.-C. Biofouling in water systems-cases, causes and countermeasures. *Appl. Microbiol. Biotechnol.* **2002**, *59*, 629–640.
(6) Ridgway, H. F.; Flemming, H.-C. *Membrane Biofouling in Water Treatment Membrane Processes*; Mallevialle, J. Odendaal, P. E., Wiesner. M. R., Eds.; McGraw-Hill: New York, 1996.
(7) Hoek, E. M. V.; Elimelech, M. Cake-enhanced concentration polarization: A new fouling mechanism for salt-rejecting membranes. *Environ. Sci. Technol.* **2003**, *37*, 5581–5588.
(8) Hoek, E. M. V.; Kim, A. S.; Elimelech, M. Influence of crossflow membrane filter geometry and shear rate on colloidal fouling in reverse osmosis and nanofiltration separations. *Environ. Eng. Sci.* **2002**, *19*, 357–372.
(9) Herzberg, M.; Elimelech, M. Biofouling of reverse osmosis membranes: Role of biofilm-enhanced osmotic pressure. *J. Membr. Sci.* **2007**, *295*, 11–20.
(10) Huertas, E.; Herzberg, M.; Oron, G.; Elimelech, M. Influence of biofouling on boron removal by nanofiltration and reverse osmosis membranes. *J. Membr. Sci.* **2008**, *318*, 264–270.
(11) Chong, T. H.; Wong, F. S.; Fane, A. G. The effect of imposed flux on biofouling in reverse osmosis: Role of concentration polarization and biofilm enhanced osmotic pressure phenomena. *J. Membr. Sci.* **2008**, *325*, 840–850.
(12) Childress, A. E.; Elimelech, M. Relating nanofiltration membrane performance to membrane charge (electrokinetic) characteristics. *Environ. Sci. Technol.* **2000**, *34*, 3710–3716.
(13) Combe, C.; Molis, E.; Lucas, P.; Riley, R.; Clark, M. M. The effect of CA membrane properties on adsorptive fouling by humic acid. *J. Membr. Sci.* **1999**, *154*, 73–87.
(14) Li, Q.; Xu, Z.; Pinnau, I. Fouling of reverse osmosis membranes by biopolymers in wastewater secondary effluent: Role of membrane surface properties and initial permeate flux. *J. Membr. Sci.* **2007**, *290*, 173–181.
(15) Bellona, C.; Drewes, J. E.; Xu, P.; Amy, G. Factors affecting the rejection of organic solutes during NF/RO treatment—A literature review. *Water Res.* **2004**, *38*, 2795–2809.
(16) Nilson, J. A.; Digiano, F. A. Influence of NOM composition on nanofiltration. *J. Am. Water Works Assoc.* **1996**, *88*, 53–66.
(17) Ang, W. S.; Elimelech, M. Protein (BSA) fouling of reverse osmosis membranes: Implications for wastewater reclamation. *J. Membr. Sci.* **2007**, *296*, 83–92.
(18) Ang, W. S.; Elimelech, M. Fatty acid fouling of reverse osmosis membranes: Implications for wastewater reclamation. *Water Res.* **2008**, *42*, 4393–4403.
(19) Ang, W. S.; Lee, S.; Elimelech, M. Chemical and physical aspects of cleaning of organic-fouled reverse osmosis membranes. *J. Membr. Sci.* **2006**, *272*, 198–210.
(20) Li, Q.; Elimelech, M. Organic fouling and chemical cleaning of nanofiltration membranes: Measurements and mechanisms. *Environ. Sci. Technol.* **2004**, *38*, 4683–4693.
(21) Tang, C. Y.; Kwon, Y.-N.; Leckie, J. O. Fouling of reverse osmosis and nanofiltration membranes by humic acid--Effects of solution composition and hydrodynamic conditions. *J. Membr. Sci.* **2007**, *290*, 86–94.
(22) Seidel, A.; Elimelech, M. Coupling between chemical and physical interactions in natural organic matter (NOM) fouling of nanofiltration membranes: implications for fouling control. *J. Membr. Sci.* **2002**, *203*, 245–255.
(23) Kang, S.; Asatekin, A.; Mayes, A. M.; Elimelech, M. Protein antifouling mechanisms of PAN UF membranes incorporating PAN-g-PEO additive. *J. Membr. Sci.* **2007**, *296*, 42–50.
(24) Ostuni, E.; Chapman, R. G.; Holmlin, R. E.; Takayama, S.; Whitesides, G. M. A survey of structure-property relationships of surfaces that resist the adsorption of protein. *Langmuir* **2001**, *17*, 5605–5620.
(25) Park, N.; Kwon, B.; Kim, I. S.; Cho, J. Biofouling potential of various NF membranes with respect to bacteria and their soluble microbial products (SMP): Characterizations, flux decline, and transport parameters. *J. Membr. Sci.* **2005**, *258*, 43–54.
(26) Hong, S.; Elimelech, M. Chemical and physical aspects of natural organic matter (NOM) fouling of nanofiltration membranes. *J. Membr. Sci.* **1997**, *132*, 159–181.
(27) Fonseca, A. C.; Summers, R. S.; Greenberg, A. R.; Hernandez, M. T. Extra-cellular polysaccharides, soluble microbial products, and natural organic matter impact on nanofiltration membranes flux decline. *Environ. Sci. Technol.* **2007**, *41*, 2491–2497.
(28) Flemming, H.-C. Reverse osmosis membrane biofouling. *Exp. Therm. Fluid Sci.* **1997**, *14*, 382–391.
(29) Kim, A. S.; Chen, H.; Yuan, R. EPS biofouling in membrane filtration: An analytic modeling study. *J. Colloid Interface Sci.* **2006**, *303*, 243–249.
(30) Li, Q.; Elimelech, M. Synergistic effects in combined fouling of a loose nanofiltration membrane by colloidal materials and natural organic matter. *J. Membr. Sci.* **2006**, *278*, 72–82.
(31) Liu, H.; Fang, H. H. P. Extraction of extracellular polymeric substances (EPS) of sludges. *J. Biotechnol.* **2002**, *95*, 249–256.
(32) Vrijenhoek, E. M.; Hong, S.; Elimelech, M. Influence of membrane surface properties on initial rate of colloidal fouling of reverse osmosis and nanofiltration membranes. *J. Membr. Sci.* **2001**, *188*, 115–128.
(33) Herzberg, M.; Elimelech, M. Physiology and genetic traits of reverse osmosis membrane biofilms: A case study with *Pseudomonas aeruginosa*. *ISME J.* **2008**, *2*, 180–194.
(34) Dubois, M.; Gilles, K. A.; Hamilton, J. K.; Rebers, P. A.; Smith, F. Colorimetric method for determination of sugars and related substances. *Anal. Chem.* **1956**, *28*, 350–356.
(35) Frolund, B.; Palmgren, R.; Keiding, K.; Nielsen, P. H. Extraction of extracellular polymers from activated sludge using a cation exchange resin. *Water Res.* **1996**, *30*, 1749–1758.
(36) Turakhia, M. H.; Characklis, W. G. Activity of *Pseudomonas aeruginosa* in biofilms: Effect of calcium. *Biotechnol. Bioeng.* **1989**, *33*, 406–414.
(37) Lee, S.; Elimelech, M. Relating organic fouling of reverse osmosis membranes to intermolecular adhesion forces. *Environ. Sci. Technol.* **2006**, *40*, 980–987.
(38) Garcia-Molina, V.; Esplugas, S.; Wintgens, T.; Melin, T. Ultrafiltration of aqueous solutions containing dextran. *Desalination* **2006**, *188*, 217–227.
(39) Nguyen, T. H.; Elimelech, M. Plasmid DNA adsorption on silica: Kinetics and conformational changes in monovalent and divalent salts. *Biomacromolecules* **2007**, *8*, 24–32.

ES900087J